Editor's choice paper

Catalytic isomerization of hydrophobic allylarenes in aqueous microemulsions

Diana Meltzer[a], David Avnir[a], Monzer Fanun[b], Vitaly Gutkin[c], Inna Popov[c], Reinhard Schomäcker[d], Michael Schwarze[d], Jochanan Blum[a,*]

[a] Institute of Chemistry, The Hebrew University, Jerusalem 91904, Israel
[b] Center for Colloids and Surface Research, Al-Quds University, East Jerusalem 51000, Palestinian Authority
[c] Center for Nanoscience and Nanotechnology, The Hebrew University, Jerusalem 91904, Israel
[d] Institut für Chemie, Technische Universität Berlin, Strasse des 17. Juni 124, D-10623 Berlin, Germany

ARTICLE INFO

ABSTRACT

In the course of our attempts to replace the traditional but environmentally disfavored organic solvents in organic processes by water, we studied the double bond isomerization of hydrophobic allylarenes, in aqueous microemulsions. The catalyst for these reactions was the rhodium-trichloride-Aliquat® 336 ion pair encaged within hydrophobic silica sol–gel. During the entrapment of the rhodium compound, it was converted into supported catalytically active Rh(0) nanoparticles characterized by TEM and XPS studies. The transformations of the allylarenes to (E)- and (Z)-1-phenyl-1-propenes follows the first order rate law, and proved to be significantly affected by the electronic nature of the substrates and by the hydrophobicity of the sol–gel support. Upon completion of the isomerization the catalyst could be recovered and recycled at least six times without a decrease in the catalytic activity after the first catalytic run.

© 2010 Elsevier B.V. All rights reserved.

1. Introduction

In the course of the attempts to replace harmful solvents used in organic synthesis by water [1,2] we have developed a three phase emulsion/solid state transport system (EST) that enables us to perform hydrogenation [3,4], hydroformylation [5] and C–C coupling reactions of water insoluble substrates in aqueous media by recyclable transition metal catalysts [6,7]. We now find that the EST system is also applicable to catalytic isomerization of hydrophobic olefins. A variety of industrially important processes involve double bond migration reactions [8]. Examples are the syntheses of various fatty acids, terpenes, alkaloids, and steroids. Double bond isomerization is also a key step in the higher olefin manufacturing processes and in the fabrication of various fragrances [9]. As a model reaction we chose the double bond migration in allylarenes that gives ultimately equilibrium mixtures of (E)- and (Z)-1-propenylarenes shown in Scheme 1. Our studies revealed several differences between the isomerization pathways in some organic solvents and in aqueous microemulsions.

2. Experimental

2.1. Instruments

NMR spectra were recorded with either a Bruker DRX-400 or a Bruker Avance II-500 in CDCl₃, Infrared spectra were obtained with a Bruker Vector 22-FTIR spectrometer. Mass spectral measurements were performed with a Q-TOF-II spectrometer. ICP-MS analyses were performed with a Perkin-Elmer model ELAN DRC II instrument. A Micrometric ASAP 2020 instrument was used for BET-N₂, and BTH-N₂ surface area and pore diameter measurements of the sol–gel matrices. Analytical gas chromatographic determinations were carried out with a Hewlett–Packard model Agilent 4890 D by using a 30 m long column packed with Carbowax 20M-poly(ethylene glycol) in fused silica (Supelco 25301-U). Preparative gas chromatographic separations were performed on a Varian Aerograph instrument series 1400 equipped with a 2 m long 10% Carbowax on Chromosorb W column. XPS measurements were performed with a Kratos Axis Ultra X-ray photoelectron spectrometer. Spectra were acquired with monochromated Al K$_\alpha$ (1486.7 eV) X-ray source with 0° take off angle. The pressure in the test chamber was maintained at 1.5×10^{-9} Torr during the acquisition process. High resolution XPS scans were collected for Rh 3d and C 1s peaks with pass energy 20 eV. The XPS binding energy was calibrated with respect to the peak position of C 1s at 285.0 eV. Data analy-

* Corresponding author. Tel.: +972 2 6585329; fax: +972 2 6513832.
  E-mail address: jblum@chem.ch.huji.ac.il (J. Blum).
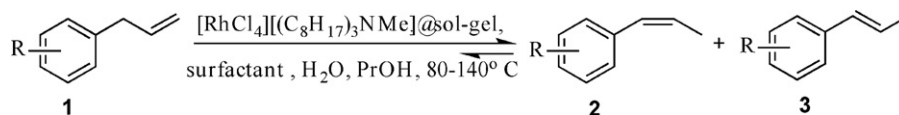
Scheme 1.

sis was performed with Vision processing data reduction software (Kratos Analytical Ltd.) and Casa XPS (Casa Software, Ltd.). Transmission electron microscopy was done with Scanning Transmission Electron Microscope (STEM) Tecnai G^2 F20 (FEI Company, USA) operated at 200 kV and equipped with EDAX-EDS for identification of the elemental composition. Initial powders were dispersed in ethanol and dropped onto a standard 400 mesh carbon coated copper TEM grid. The average particle size of the sol–gel entrapped $RhCl_3$-Aliquat 336 was measured with an Olympus CX31 light microscope operated at the magnification of 40.

2.2. Chemicals

Tetramethoxysilane (TMOS), *n*-propyltrimethoxysilane, *n*-octyltriethoxysilane and phenyltriethoxysilane were obtained from ABCR-Glest, Inc. Allylbenzene, 4-allylanisole, methyltrioctyl-lammonium chloride (Aliquat 336), cetyltrimethylammonium bromide (CTAB), and rhodium trichloride trihydrate were purchased from Sigma–Aldrich Chemical Company. Sodium dodecyl sulfate (SDS) was obtained from Ridel de Haën; C_{12}–C_{14} alcohols polyoxyethylene ethers (Marlipal 24/70) were purchased from Sasol Co. and sucrose laurate (L-1695-) from Mitsubishi-Kasai Food Corp., Mie, Japan. 4-Allyltoluene, and 4-allylchlorobenzene were prepared from allyl bromide and the corresponding bromoarenes [10]. (*E*)- and (*Z*)-1-phenyl-1-propene, 1-(4-tolyl)-1-propene, 1-(4-methoxyphenyl)-1-propene and 1-(4-chlorophenyl)-1-propene were prepared from the corresponding allylarenes by polystyrene-bound dichlorobis(triphenylphosphine) ruthenium (II) [11] followed by gas chromatographic separation of the isomers.

2.3. Preparation of the sol–gel entrapped rhodium catalyst

A mixture of phenyltrimethoxysilane (0.45 ml, 2.26 mmol), TMOS (3.6 ml, 24.2 mmol), $RhCl_3 \cdot 3H_2O$ (30 mg. 0.114 mmol) dissolved in triply distilled water (TDW, 2.0 ml), and Aliquat 336 (50 mg, 0.124 mmol) dissolved in MeOH (3.0 ml), was stirred at room temperature for as long as possible (usually ca. 3 d). The gel was allowed to stand at 25 °C for 3 d and then dried at 80 °C and 0.5 Torr for 24 h. The dry sol–gel matrix was washed and sonicated with boiling CH_2Cl_2 (30 ml) and redried at 0.5 Torr at 80 °C for 5 h before use. Both the ceramic material and the combined washings were analyzed for their rhodium content by ICP-MS. In none of the experiments did the washing contain >0.02 mg Rh.

For the entrapment of the $RhCl_3$-Aliquat 336 ion pair within octylated or propylated sol–gel, the hydrolysis of the TMOS and of the alkyltrialkoxysilanes were carried out separately. The hydrolysis of octyltriethoxysilane (2.4 ml, 6.68 mmol) was performed with EtOH (5.6 ml) and TDW (0.4 ml), and the hydrolysis of propyltrimethoxysilane (1.17 ml, 6.64 mmol) was carried out with MeOH (3.88 ml) and TDW (0.4 ml). After 24 h, TMOS (3.6 ml, 24.2 mmol) together with $RhCl_3 \cdot 3H_2O$ (30 mg, 0.114 mmol) dissolved in TDW (2.0 ml) and Aliquat 336 (50 mg, 0.124 mmol) in MeOH (2.4 ml) was added to each of the hydrolyzed silanes.

2.4. Preparation of the microemulsions

A mixture of the allylarene (1.35 mmol), TDW (17–20 ml), the appropriate surfactant (0.6–0.8 g and *n*-PrOH (1.6–2.0 ml) was

stirred magnetically at 25 °C until a clear transparent microemulsion was formed. In some cases the addition of a few drops of the propanol was necessary.

2.5. General procedure for the catalytic isomerization

One half of the above immobilized rhodium catalyst (containing usually 0.057 mmol of the rhodium compounds) was roughly ground and admixed within a mini autoclave equipped with a sampler together with one of the aforementioned freshly prepared microemulsions. The autoclave was inserted in a preheated thermostat. After stirring the reaction mixture at the desired temperature, and for the necessary length of time, the autoclave was cooled to 20 °C. The sol–gel material was filtered off, washed and sonicated first for 30 min with TDW (30 ml) and then with hexanes. The sol–gel-free filtrate was treated with NaCl (2 g), which caused breakage of the microemulsion and phase separation. The aqueous layer was extracted with hexanes (2 × 30 ml), the extract was dried over $MgSO_4$, concentrated and subjected to gas chromatographic separation and analysis. Both the recovered sol–gel material and the liquid phases were analyzed for Rh by ICP-MS. The dried sol–gel was reused in a further catalytic run. Isomerization experiments in several organic solvents were performed for comparison essentially as described in the literature [12].

3. Results and discussion

Previously [12] we reported that catalytic double bond migration in allylic compounds by sol–gel entrapped $[(C_8H_{17})_3NCH_3][RhCl_4]$ ($RhCl_3$-Aliquat 336) takes place smoothly in toluene at 90 °C. After completion of the process the orange colored support could be recycled. Unless a hydrophilic catalyst was employed [13], the replacement of the organic solvent by water proved to stall the isomerization, but addition of a surfactant, together with an alcoholic co-surfactant, resumed the catalytic process. In the aqueous medium the sol–gel supported catalyst turns black. TEM analysis indicated that this black sol–gel contains Rh(0) nanoparticles (vide infra). XPS measurements of the ceramic material revealed that prior to the catalytic process, i.e., the immobilized $[(C_8H_{17})_3NCH_3][RhCl_4]$, the rhodium catalyst was in the +3 oxidation state showing binding energy (BE) peaks at 308.67 and 313.41 eV corresponding to Rh(III) $3d_{5/2}$ and Rh(III) $3d_{3/2}$, respectively (cf. e.g., Refs. [14–16]). After the isomerization process, the major BE peaks were centered at 307.62 and 312.36 eV, [Rh(0) $3d_{5/2}$ and Rh(0) $3d_{3/2}$] having shoulders at ~308 and ~312 eV [that corresponds to Rh(I) $3d_{5/2}$ and Rh(I) $3d_{3/2}$] and show distorted curves at 309 and 313 eV. The shoulders and distorted curves indicate the presence of residual traces of Rh(I) and Rh(III) species that are buried within the bulk sol–gel material, and, therefore are not converted into Rh(0) nanoparticles. The XPS analysis of the used heterogenized catalyst recovered from the isomerization in toluene did not have any peaks that correspond to Rh(0). The only signals were those of Rh(I) $3d_{5/2}$, Rh(I) $3d_{3/2}$, Rh(III) $3d_{5/2}$ and Rh(III) $3d_{3/2}$. This means that the reaction in toluene does not involve the formation of metallic nanoparticles.

In analogy to the isomerization of allylbenzenes by heterogenized catalysts in organic solvents [12,17–19] the reactions in microemulsions were also converted after prolonged heating into equilibrium mixtures of **1**, **2** and **3**, in which the residual compo-

Table 1
Isomerization of allylbenzene by immobilized $RhCl_3$-Aliquat 336 in microemulsion under comparable experimental conditions[a].

Entry	Hydrophobic function R[b]	Composition of reaction mixture after 3 h, %[c,d]		
		1, R = H	**2, R = H**	**3, R = H**
1	None	26.6	8.6	64.8
2	Phenyl	46.0	4.0	50.0
3	n-Octyl	5.8	8.5	85.7
4	n-Propyl	3.9	7.5	88.6

[a] *Reaction conditions*: Microemulsion of 1 (0.18 ml), SDS (0.65 g), n-PrOH (1.63 ml), H_2O (17.6 ml), sol–gel material prepared from tetramethoxysilane (TMOS, 1.8 ml), either $RSi(OMe)_3$ or $RSi(OEt)_3$ (7 mmol), $RhCl_3 \cdot 3H_2O$ (15 mg), $[(C_8H_{17})_3NCH_3]Cl$ (25 mg), 140 °C.
[b] In $RSi(OR')_3$.
[c] Average of at least two reactions that did not differ by ±3%.
[d] In the first run.

Table 2
Substituent effect on the isomerization of allylbenzenes 1 by the heterogenized $RhCl_3$-Aliquat 336 under the EST conditions[a].

| Entry	Substituent, R	10^5 M s^{-1}	k_s/k_a	$\log(k_s/k_a)$[b]
1	H	5.74	1	0
2	4-Cl	2.64	0.460	−0.337
3	4-CH_3	10.51	1.831	0.263
4	4-OCH_3	13.08	2.279	0.358

[a] Reaction conditions as in Table 1 with phenylated sol–gel support.
[b] k_a and k_s represent the reaction constants for the consumption of the unsubstituted and of the substituted allylbenzene, respectively.

nent **1** exists only in a small amount. When for example, the starting unsaturated hydrocarbon was **1, R = H**, a mixture of 0.9% of **1**, 7.5% **2** and 91.6% of **3** was generated after 20 h at 140 °C. However, unlike in toluene the reactions in microemulsions were found to always form Rh(0) nanoparticles.

The fact that both the Rh(III) precatalyst and the Rh(0) catalyze (in organic media) the double bond migration in allylarenes, gave rise to the question whether both species independently promote the isomerization process in the microemulsion. As we have previously observed, the catalytically active $RhCl_3$-Aliquat 336 can be extracted from the sol–gel support with hot ethanol [20], we treated our immobilized catalyst with the boiling alcohol after the second, third and fourth run and found no Rh(III) species in any of the extracts. Therefore, we conclude that unlike in toluene, under the EST conditions only the Rh(0) nanoparticles are responsible for the catalytic reactions.

It should be noted that although the generation of metallic nanoparticles during isomerization of olefins is much less common than during a variety of other catalytic processes [21], the double bond migration in some cycloalkenes by Ni/Sn catalysts can be regarded as a nanoparticle-catalyzed process [22].

In analogy to some other catalyses that take place under the EST conditions [4,23], the isomerization of allylbenzene proved to depend strongly on the hydrophobicity of the sol–gel support. The hydrophobic sol–gel matrices were prepared by hydrolysis and co-condensation of TMOS and $RSi(OR')_3$, where R is the hydrophobic group and R' is either CH_3 or C_2H_5. Under comparable experimental conditions using (i) hydrophilic, (ii) phenylated, (iii) octylated and (iv) propylated sol–gel, the rates of the double bond migration were in the order of iv > iii > i > ii (see Table 1). This order is different than the one recorded in Pd(OAc)$_2$-catalyzed Heck coupling of bromobenzene and styrene in microemulsions where the reaction does not take place at all by the catalyst within the non-hydrophobic support and the best results are obtained within phenylated sol–gel [23]. It is notable that in toluene the isomerization of allylarenes by $[(C_8H_{17})_3NCH_3][RhCl_4]$ proceeds within hydrophilic sol–gel [12,20].

Under the conditions of Table 1 the catalytic transformation of allylbenzene (**1, R = H**), as well as the conversions of the substituted analogs, **1, R = Cl**; **1, R = CH$_3$** and **1, R = OCH$_3$**, follow the first order rate law, and the initial rates were found to depend on the electronic nature of the substrates. Electron donating moieties proved to enhance the rate and visa versa electron attracting groups. Representative numerical data are summarized in Table 2, and can be expressed in terms of a Hammett plot with $\rho = -1.42$ shown in Fig. 1.

Although double bond migration in allylarenes by the $RhCl_3$-Aliquat 336 catalyst, under the EST conditions, and in toluene take

place with and without formation of Rh(0) particles, respectively, the Hammett plots of both reactions (as well as by the $RhCl_3$-Dowex® 1 catalyzed process in 92% aqueous EtOH) are quite similar having σ values of the same order of magnitude [19].

The reason for the generation of Rh(0) nanoparticles in the aqueous microemulsion is not yet fully understood. In attempts to elucidate possible factors that may be responsible for the conversion of the immobilized Rh(III) into Rh(0) species in the *aqueous* medium, we first omitted the PrOH co-surfactant from the reaction mixture. However, the removal of the alcohol (which caused the isomerization to slow down) still gave sol–gel entrapped Rh(0) particles. On the other hand, experiments in *toluene*, in the presence of large quantities of propanol, did not form any nanoparticles even after prolonged heating at 140 °C within an autoclave. The possibility that the unsaturated substrate is responsible for the generation of the nanoparticles, has also been disproved. The latter particles were formed equally well when the allylbenzene was replaced by either benzene, toluene or propylbenzene. Similar Rh(0) particles appeared in the TEM micrographs when the isomerization was conducted under ambient atmosphere or under N_2.

The presence of surfactants in the reaction mixture led nearly always to the generation of Rh(0) particles. An exception was the case in which allylbenzene (**1, R = H**) was isomerized in toluene under anhydrous conditions and the surfactant was the toluene soluble Marlipal 24/70 (vide infra). Nanoparticles started, however, to accumulate upon addition of water to the stirred reaction mixture. Thus, we assume that the *aqueous* surfactant is the main reducing factor (cf., e.g. Ref. [24]). Although we have no means for quantitatively measuring the amount of the randomly distributed nanoparticles, we observed that both their abundance and the size
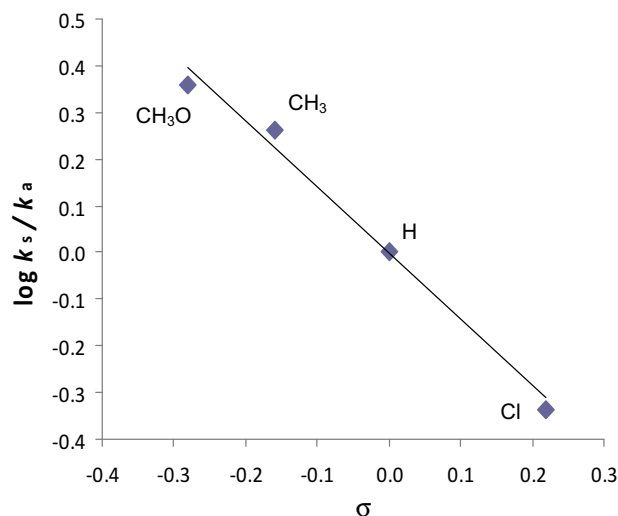
Fig. 1. Hammett plot for the isomerization reaction shown in Scheme 1 using $[(C_8H_{17})_3NCH_3][RhCl_4]$ in phenylated silica sol–gel at 140 °C as pre-catalyst. k_a and k_b are the same as in Table 2. The σ values were taken from Ref. [28]; $Y = -1432X$; $R^2 = 0.9891$.
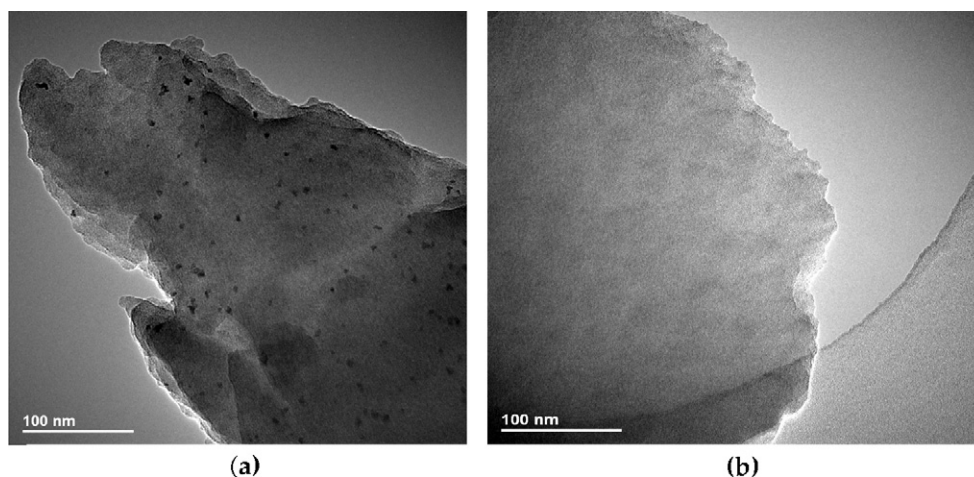
Fig. 2. TEM images of typical sol–gel supported sections after isomerization of allylbenzene by the $[(C_8H_{17})_3NCH_3][RhCl_4]$ at sol–gel pre-catalyst: (a) in an aqueous microemulsion, (b) in toluene.

are strongly dependent on the reaction temperature. TEM measurements indicated that during the isomerization of **1**, **R = H** at 140 °C densely distributed Rh(0) particles, having diameters of 2–5 nm are formed (see Fig. 2), but at 100 °C their amount was significantly reduced and their size shrunk to 0.7–1.7 nm. At 82 °C both the formation of nanoparticles and the isomerization proceeded very slowly. Seven days were required to obtain a mixture of 3.7% of **1**, **R = H**, 6.8% of **2**, **R = H** and 89.5% of **3**, **R = H**.

The nanoparticles seem to be formed equally well when the surfactant is anionic (SDS), non-ionic [e.g., Marlipal® 24/70 or sucrose laurate (L 1695)] or cationic [cetyltrimethylammonium bromide, (CTAB)]. The nature of the surfactant has however, a different influence on the efficiency of the catalytic isomerization. Some typical conversions of allylbenzene by the Rh(0) nanoparticles in microemulsions stabilized in the presence of SDS, Marlipal 24/70, L 1695 or CTAB during 3 h at 140 °C, under comparable standard reaction conditions, are summarized in Table 3. These data can be rationalized by the different tendency of the surfactant micelles to be absorbed by the catalyst-containing sol–gel. While the anionic SDS is actually repelled by the partially negatively charged silica sol–gel, the cationic CTAB is attracted by the ceramic material [25,26].

The heterogenization of the $[(C_8H_{17})_3NCH_3][RhCl_4]$ ion pair precatalyst by its entrapment within silica sol–gel, makes the catalyst recyclable, indifferently if it acts in the form of a discrete organometallic complex in toluene [12] or as supported Rh(0) nanoparticles in aqueous microemulsions (Table 4). A significant loss of catalytic activity takes place only in the first run. We assume that this decrease in activity is associated with some morphological changes in the sol–gel matrix (Si–O bond breaking) that takes place at 140 °C by the water. Support for this assumption is provided by the BET measurements of the internal surface areas and

Table 3
Effect of the nature of the surfactant on the isomerization of allylbenzene[a].

Entry	Surfactant	Composition of reaction mixture after 3 h, %[b]		
		1, R = H	**2**, R = H	**3**, R = H
1	SDS	46	4	50
2	Marlipal 24/70	27	8	65
3	L 1695	35	5.5	59.5
4	CTAB	17	11.5	71.5

[a] Reaction conditions as in Table 1 except that the hydrophobic function was phenyl and the surfactant was as indicated.
[b] In the first run.

Table 4
Dependence of the isomerization of allylbenzene in aqueous microemulsion on the recycling of the catalyst[a].

Run No.	Yield after 3 h, %[b]		
	1, R = H	**2**, R = H	**3**, R = H
1	46	4	50
2	70	3	27
3	71	4	25
4	74	3	23
5	73	4	24

[a] Reaction conditions as in Table 1, except that the sol–gel material was formed in all cases from TMOS and PhSi(OEt)$_3$.
[b] The yields are the average of 2–5 experiments that did not differ by more than ±2%.

the sizes of the pore diameters. The initial average internal surface area of 264 m^2/g was found to grow to 335 m^2/g after the fifth catalytic cycle. Likewise, the average pore diameter extended from 21 to 32 Å (cf. a similar size increase during the Heck reaction in water [6]). We recall that in toluene and in some other organic solvents, the isomerization catalyst $[(C_8H_{17})_3NCH_3][RhCl_4]$ (entrapped in hydrophilic sol–gel) also loses some of its catalytic activity. However, the decrease in organic solvents was shown to be associated with pore entrance blocking by the substrate and products [20]. There the addition of a limited amount of water helps to reopen the clogged pores, but addition of excessive water during the catalytic process inhibits the isomerization.

In many catalytic reactions, mass-transport-limitations have a strong impact on the reaction rate. Here, in the EST system, the reaction takes place at the rhodium nanoparticles that are entrapped in a porous hydrophobic sol–gel matrix. The allylbenzene or the substituted analogs, dissolved in normal micelles of an o/w-microemulsion, must be transported from the aqueous environment to the active site of the catalyst. A scheme of this process is shown in Fig. 3.

The Weisz–Prater criterion (Eq. (1)) [27] which is based on macrokinetics and use to estimated the influence of diffusion on the reaction rate by a calculation of the ratio of the characteristic reaction time to the characteristic diffusion time is the Weisz module Ψ. For Ψ-values lower than 1 the influence of diffusion can be neglected.

$$\Psi = \frac{((n+1)/2)((r \cdot \rho_{cat})/c_0)}{D_{eff}/L_c^2} \tag{1}$$
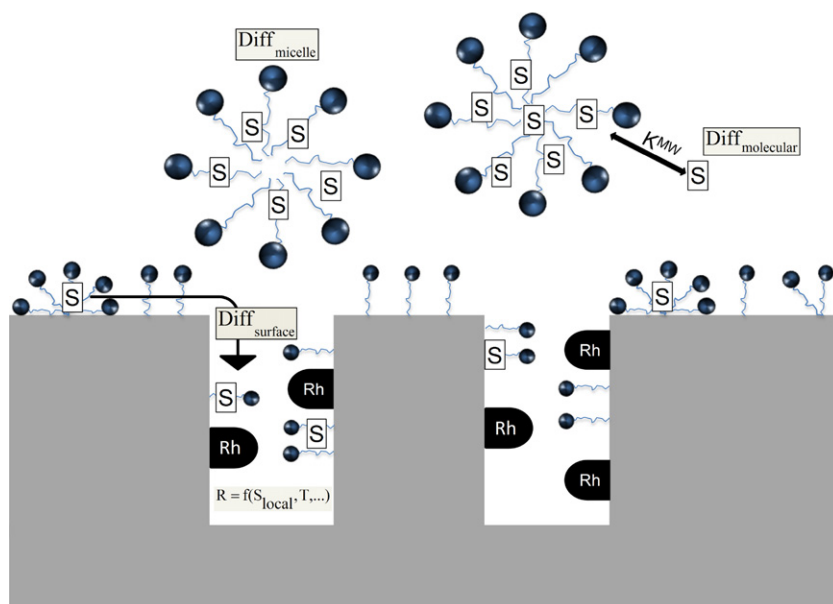
Fig. 3. Possible transport mechanism in the EST system (S: substrate, Rh: rhodium nanoparticles). K^{MW} is the partition coefficient between the micelles and the continuous aqueous phase and Diff stands for diffusion. The reaction rate R is a function of the experimental conditions, e.g. temperature, and depends on the local substrate concentration.

In Eq. (1), L_c (cm) is the characteristic catalyst length, n is the reaction order, r (mol s^{-1} g^{-1}) is the reaction rate, ρ_{cat} (g/cm^3) is the density of the catalyst, D_{eff} (cm^2/s) is the effective diffusion coefficient and c_0 (mol/l) is the initial substrate concentration, respectively. From light microscope measurements a mean characteristic catalyst length of 0.063 cm is obtained for the sol–gel material that has a density of approximately 1.9 g/cm^3. From the isomerization experiments, the reaction order was found to be 1 and a reaction rate of 7.8×10^{-8} mol s^{-1} g^{-1} was calculated for an initial concentration of 0.068 mol/l of **1**. Based on these values, Ψ was calculated for different situations: molecular diffusion and micelle diffusion. For micelle diffusion ($D_{eff} \sim 10^{-9} - 10^{-7}$ cm^2/s) the Weisz module would be extremely large ($\Psi \sim 100$–10,000) but in case of molecular diffusion ($D_{eff} \sim 10^{-5}$ cm^2/s) values lower than one will be obtained and mass transfer limitations can be excluded. This estimation shows that the substrate is not able to approach the catalyst by transportation through micelles, therefore a diffusion of the individual substrate molecules is the only possible transport mechanism. This is supported by the observation that the rate responds to the effect of the substituents. In case of mass transport limitations this behavior should not be observed. The partition coefficient K^{MW} of the allylbenzene between the micelles and

the continuous aqueous phase has a substantial influence on this molecular diffusion process. This parameter itself is again strongly affected by the size and polarity of the surfactants.

Comparison of the isomerization of allylbenzene in aqueous microemulsions with that in organic solvents at identical temperatures and stirring rates, with the same substrate concentration and in the presence of the same amount of heterogenized precatalyst reveals, that the reaction in the aqueous medium is the more efficient one. However, it should be changed to noted, that while in the reaction in the organic solvent no surfactant is present, and the sol–gel matrix is hydrophilic, under the EST conditions these components of the systems play a significant role. Some representative experiments carried out in different solvents are summarized in Table 5.

4. Conclusions

In aqueous microemulsions the sol–gel entrapped ion pair $[(C_8H_{17})_3NCH_3][RhCl_4]$ decomposes into Rh(0) nanoparticles. In benzene and toluene no such decomposition could be detected, although allylarenes were found to undergo isomerization to 1-aryl-1-propenes in both types of solvents. The reductive transformation of the Rh(III) pre-catalyst to the Rh(0) species seems to be affected by the aqueous surfactant that is used to solubilize the hydrophobic allylarene. The efficiency of the double bond migration in water is dependent on both the electronic nature of the allylic substrate and that of the surfactant, as well as on the hydrophobicity of the sol–gel matrix in which the rhodium is encaged. It can be concluded that no mass transfer process inhibits the reaction in the studied EST system. Since the reaction in the aqueous medium proceeds faster than in benzene and in toluene, the double bond isomerization, under EST conditions, can be useful for the replacement of the conventional organic solvent by water.

Table 5
Dependence of the isomerization on the reaction medium[a].

Entry	Reaction medium	Time (h)	Composition of reaction mixture after 3 h, %[b]			Formation of metallic nanoparticles
			1, R = H	2, R = H	3, R = H	
1	Aq. microemulsion	14.5	7.9	7.1	85.0	+
2	Aq. microemulsion	20[c]	0.9	7.6	91.5	+
3	THF	14.5	77.0	2.9	20.1	+
4	Benzene	14.5	88.6	2.9	8.5	−
5	Toluene	14.5	75.0	5.5	19.5	−

[a] Reaction conditions for entries 1 and 2 as in Table 1. Conditions for entries 3–5: allylbenzene (0.18 ml), solvent (18 ml), sol–gel material from TMOS (1.8 ml), PhSi(OMe)$_3$ (0.225 ml), RhCl$_3$·3H$_2$O (15 mg) and $[(C_8H_{17})_3NCH_3]$Cl (25 mg), 140 °C.
[b] In the first run.
[c] Since an increase of the reaction time did not affect anymore the composition of the reaction mixture we postulate that the given data are those of the equilibrium mixture.

References

[1] W. Wei, C.C.K. Keh, C.-J. Li, R.S. Varma, Chem. Technol. Environ. Policy 6 (2004) 250–257, and references cited therein.
[2] U.M. Lindström (Ed.), Organic Reactions in Water: Principles Strategies and Applications, Blackwell, Oxford, 2007.
[3] R. Abu-Reziq, D. Avnir, J. Blum, Angew. Chem. Int. Ed. 41 (2002) 4132–4134.
[4] R. Abu-Reziq, J. Blum, D. Avnir, Chem. Eur. J. 10 (2004) 958–962.
[5] R. Abu-Reziq, D. Avnir, J. Blum, Eur. J. Org. Chem. (2005) 3640–3642.
[6] D. Tsvelikhovsky, J. Blum, Eur. J. Org. Chem. (2008) 2417–2422.
[7] D. Tsvelikhovsky, D. Pessing, D. Avnir, J. Blum, Adv. Synth. Catal. 350 (2008) 2856–2858.
[8] W.A. Herrmann, M. Prinz, in: B. Cornils, W.A. Herrmann (Eds.), Applied Homogeneous Catalysis with Organometallic Compounds, Wiley-VCH, Weinheim, Germany, 2002, pp. 1119–1130.
[9] A. Scarso, M. Colladon, P. Sgarbossa, C. Santo, R.A. Michelin, G. Strukul, Organometallics 29 (2010) 1487–1497, and references cited therein.
[10] C.D. Hurd, M.T. Bollman, J. Am. Chem. Soc. 56 (1934) 447–449.
[11] A. Zoran, Y. Sasson, J. Blum, J. Org. Chem. 46 (1981) 255–260.
[12] J. Blum, A. Rosenfeld, N. Polak, O. Israelson, H. Schumann, D. Avnir, J. Mol. Catal. A: Chem. 107 (1996) 217–223.
[13] H. Schumann, V. Ravindar, L. Meltser, W. Baidossi, Y. Sasson, J. Blum, J. Mol. Catal. A: Chem. 118 (1997) 55–61.
[14] J.L.G. Fierro, J.M. Palacios, F. Tomas, Surf. Interface Anal. 13 (1988) 25–32.
[15] V.I. Nefedov, M.N. Firsov, I.S. Shaplygin, J. Electron Spectrosc. Relat. Phenom. 26 (1982) 65–79.
[16] C. Furlani, G. Mattogno, G. Polzonetti, G. Braca, G. Valentini, Inorg. Chim. Acta 69 (1983) 199–205.
[17] A. Zocan, Y. Sasson, J. Blum, J. Org. Chem. 46 (1981) 255–260.
[18] M. Setty-Fichman, J. Blum, Y. Sasson, M. Eisen, Tetrahedron Lett. 35 (1994) 781–784.
[19] M. Setty-Fichman, Y. Sasson, J. Blum, J. Mol. Catal. A: Chem. 126 (1997) 27–36.
[20] A. Rosenfeld, D. Avnir, J. Blum, J. Chem. Soc., Chem. Commun. (1993) 583–584.
[21] D. Astruc (Ed.), Nanoparticles and Catalysis, Wiley-VCH, Weinheim, Germany, 2008.
[22] P. Lesage, J.-P. Candy, C. Hirigoyen, F. Humbolt, M. Leconte, J.-M. Basset, J. Mol. Catal. A: Chem. 117 (1996) 303–309.
[23] A. Rozin-Ben Baruch, D. Tsvelikhovsky, M. Schwarze, R. Schomäcker, M. Fanun, J. Blum, J. Mol. Catal. A: Chem. 323 (2010) 65–69.
[24] M. de Dios, F. Barroso, C. Tojo, in: M. Fanun (Ed.), Surfactants Science Series, Vol. 144. Microemulsions: Properties and Applications, CRC Press/Taylor and Francis Inc., Boca Raton, 2009, pp. 451–464.
[25] C. Rottman, S. Garda, Y. De Hazan, S. Malchior, D. Avnir, J. Am. Chem. Soc. 121 (1999) 8533–8543.
[26] E. Tyrode, M.W. Rutland, C.D. Bain, J. Am. Chem. Soc. 130 (2008) 17434–17445, and references cited therein.
[27] P.B. Weisz, C.D. Prater, Adv. Catal. 6 (1954) 143–196.
[28] T. Matsui, H.C. Ko, G. Hepler, Can. J. Chem 52 (1974) 2906–2911.